C. R. Geoscience 351 (2019) 236–242

Contents lists available at ScienceDirect

Comptes Rendus Geoscience

www.sciencedirect.com

Internal Geophysics (Physics of Earth's Interior)

Elastic constants of single-crystal Pt measured up to 20 GPa based on inelastic X-ray scattering: Implication for the establishment of an equation of state

Seiji Kamada [a,b,*], Hiroshi Fukui [c,d], Akira Yoneda [e], Hitoshi Gomi [e], Fumiya Maeda [b], Satoshi Tsutsui [f], Hiroshi Uchiyama [f], Naohisa Hirao [f], Daisuke Ishikawa [f], Alfred Q.R. Baron [d]

[a] Frontier Research Institute for Interdisciplinary Sciences, Tohoku University, 6-3 Aramaki, Aoba, Sendai, 980-8578 Miyagi, Japan
[b] Department of Earth Science, Graduate School of Science, Tohoku University, 6-3 Aramaki, Aoba, Sendai, 980-8578 Miyagi, Japan
[c] Graduate School of Material Science, University of Hyogo, 3-2-1 Kouto, Kamigori, 678-1297 Hyogo, Japan
[d] Materials Dynamics Laboratory, RIKEN SPring-8 Center, RIKEN, 1-1-1 Kouto, Sayo, 679-5148 Hyogo Japan
[e] Institute for Planetary Materials, Okayama University, 827 Yamada, Misasa, 682-0193 Tottori, Japan
[f] Japan Synchrotron Radiation Research Institute (JASRI), 1-1-1 Kouto, Sayo, 679-5198 Hyogo, Japan

ARTICLE INFO

Article history:
Received 30 March 2018
Accepted after revision 9 November 2018
Available online 17 January 2019

Handled by Guillaume Fiquet

Keywords:
Primary pressure scale
Platinum
Single crystal
Inelastic X-ray scattering
Diamond anvil cell

ABSTRACT

Phonon velocities and densities for Pt were measured based on inelastic X-ray scattering from ambient pressure to 20 GPa in order to independently determine its equation of state (EOS). Phonon velocities were determined with sine dispersion relations. C_{ij} values were obtained by fitting phonon velocities and densities to the Christoffel equation. We found that the obtained C_{ij}s were in good agreement with previously reported C_{ij}s at ambient condition. Based on the C_{ij} values in various conditions, experimental pressures were calculated. The EOS of Pt as a primary pressure scale was determined based on the experimental pressures. We report $K' = 5.17$ with fixed $K_T = 274.1$ GPa and $V_0 = 60.360$ Å^3 for Vinet EOS. Our scale is in good agreement with several previously published scales based on shock experiments and XRD.

1. Introduction

Recently, high-pressure experimental techniques using a diamond anvil cell (DAC) have significantly progressed, and phase relationships of Fe and Fe-light element systems have been investigated under pressure conditions corresponding to the center of the Earth (e.g., Tateno et al., 2010, 2015). Although such experiments have been successfully performed, the interpretation of their results strongly depends on the chosen pressure scale. Sakai et al. (2014) reported that the equations of state (EOS) of hcp Fe gave different pressures depending on how they were established, and that the difference was as large as 25 GPa at 300 GPa. Therefore, well-determined pressure scales are crucial for accurate determination of experimental pressures. To calibrate a pressure scale precisely enough, one needs a precisely determined pressure standard.

Platinum (Pt) is used to determine pressure in high-pressure Earth science because it has a simple face centered cubic crystal structure and does not react easily with most Earth materials (e.g., oxides, silicates) except for metals, hydrogen, carbonates, and carbides. In addition, Pt can act as a laser absorber during laser-heated DAC experiments. Therefore, Pt conveniently enables us to heat

* Corresponding author. Department of Earth Science, Graduate School of Science, Tohoku University, 6-3 Aramaki, Aoba, Sendai, 980-8578 Miyagi, Japan.
E-mail address: seijikmd@m.tohoku.ac.jp (S. Kamada).

https://doi.org/10.1016/j.crte.2018.11.003
1631-0713/

a sample and determine the pressure at the same time. Because of its usefulness, equations of state (EOSs) of Pt as a pressure scale have been proposed based on shock (e.g., Holmes et al., 1989; Jamieson et al., 1982; Matsui et al., 2009; Yokoo et al., 2009) or static compression (e.g., Dewaele et al., 2004; Dorfman et al., 2012; Fei et al., 2007).

We summarize the previously determined pressure scales of Pt to clarify the uncertainty. Fig. 1 illustrates pressure differences at room temperature between the Pt scale by Matsui et al. (2009) and other scales. The Pt scale by Matsui is chosen as a comparison standard in Fig. 1 because their scale was based on shock compression data independent of any other pressure scales and the scale was in good agreement with static compression results. Black and blue lines in Fig. 1 represent pressures based on shock compression data and static compression data, respectively. Pressures based on Holmes et al. (1989) tend to show up to 10% higher pressures compared to the Matsui scale. Other scales based on shock compression data also give pressures higher than those obtained by Matsui et al. (2009). On the other hand, the Dewaele and Fei scales based on static compression are in good agreement with the Matsui scale. Pressures obtained by the Dorfman and Jamieson scales are similar to each other, and are higher than the Matsui scale and other scales based on the static compression data. As a result of mismatches among different Pt scales shown above, EOSs of an investigated material established using different EOSs of Pt are likely to give different pressures.

Both shock and static experiments have advantages and disadvantages with respect to the accuracy of experimental pressure determination, which may result in the discrepancy between previous studies. As Hugoniot pressures can be determined without using any pressure scales, many pressure scales of various materials were established using shock compression data (Marsh, 1980).

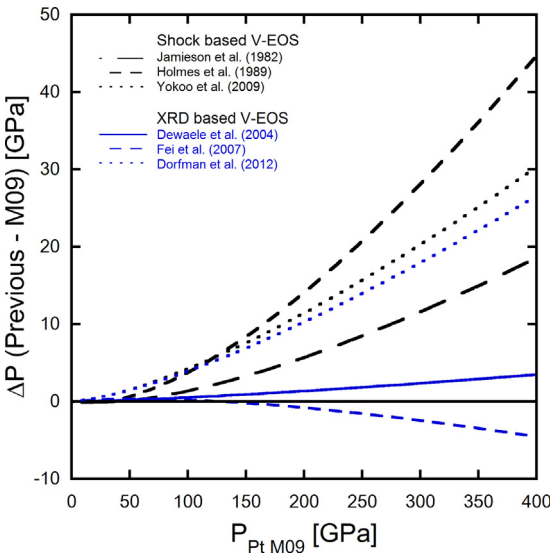

Fig. 1. Comparison of the pressure scales. Pressure differences between Matsui et al. (2009) (M09) and other scales are plotted against pressures based on Matsui et al. (2009). Black and blue lines represent scales based on shock and static compression data, respectively.

However, it is difficult to obtain isothermal pressure–volume relations due to the treatment of thermodynamics based on the Mie–Grüneisen–Debye model, a pressure dependence of the Grüneisen parameter, and an electron effect (e.g., Holmes et al., 1989; Jamieson et al., 1982; Matsui et al., 2009; Tsuchiya and Kawamura (2002); Yokoo et al., 2009). On the other hand, it is opposite for static compression experiments, since isothermal measurements can be easily performed, but they require other primary pressure standards in most of the cases.

It has been previously shown that measuring sound velocities as well as volumes or densities allows us to avoid the thermodynamic difficulty and establish an independent EOS (e.g., Yoneda et al., 2017; Zha et al., 2000). Taking this into account, we measured sound velocities and volumes of a Pt single crystal under high pressures based on inelastic X-ray scattering (IXS).

2. Methods

2.1. Experiment

The sample utilized for all IXS measurements in the present study was made from a piece of a Pt single crystal commercially purchased from MaTeck Co. The piece was cut using a focused ion beam system to the size of $20 \times 20\ \mu m^2$ with a thickness of $\sim 8\ \mu m$. A diamond anvil cell with a culet size of 400 μm was used for generating high pressures. The sample was set in a sample chamber with ruby chips as the [001] direction was normal to the culet's surface. Reference pressures were measured before and after each IXS measurement based on the Ruby scale (Zha et al., 2000). Pressure media of helium gas were loaded into the sample chamber using the gas loading system at SPring-8.

IXS measurements were performed at BL35XU of SPring-8 (Baron et al., 2000) for six different pressure points from ambient pressure to 20 GPa. The measurement at ambient pressure was performed before loading He gas into the sample chamber. Energies of incident beams were 17.794 and 21.747 keV using the Si(9 9 9) and (11 11 11), respectively. The incident beams were focused using a KB mirror setting (Ishikawa et al., 2013). The energy resolutions and beam sizes were ~3.0 meV and $13 \times 19\ \mu m^2$ for 17.794 keV, and ~1.5 meV and $12 \times 17\ \mu m^2$ for 21.747 keV. We used 17.794 keV for ambient pressure measurements and 21.747 keV for high-pressure measurements. We determined orientation matrix of Pt using (2 −2 0) and (2 0 0) reflections at ambient pressure, (2 −2 0), (2 0 0), and (3 −1 −1) reflections at high pressures, which were observed before, between, and after IXS measurements. Full widths at half maximum (FWHM) of rocking curves were less than 0.12 degrees in most of the measurements, while, at the highest pressure point, values of FWHM were at most 0.34 degrees. This indicates that the single crystal's quality was preserved up to the highest pressure in this study.

In general, one IXS spectrum has at most three pairs of lines, composed of Stokes and anti-Stokes excitation of a mode, from a single crystal in addition to the elastic line. The

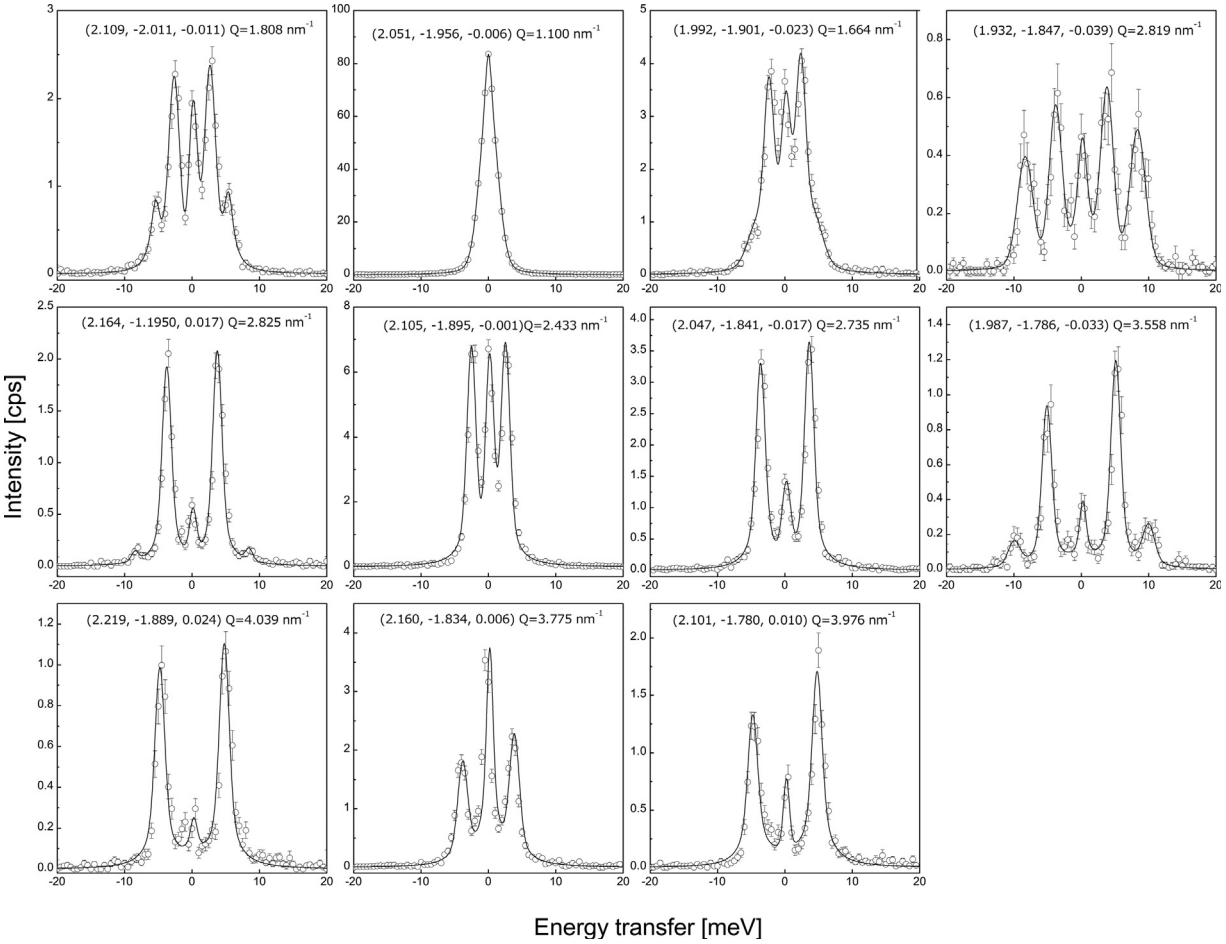

Fig. 2. Typical IXS spectra at 20 GPa. The lower right panel showed no data because of a wiring trouble at the beamline. The total momentum transfer in reciprocal lattice units is given above each spectrum. The black circles represent the observed data points with statistic errors, and the black solid curves are results of the total peak fitting.

three pairs represent one longitudinal and two transverse modes. Fig. 2 shows the typical IXS spectra obtained at highest pressure using the 12-analyzer array (Baron, 2016). The peaks were fitted using the pseudo-Voigt function and the resulting peak energies were then corrected based on the effect of finite dq values (Fukui et al., 2008). The three independent elastic constants (C_{11}, C_{12}, and C_{44}) for Pt at each experimental pressure were determined using Christoffel's equation as follows (Fukui et al., 2008):

$$\rho\ V_{\mathrm{sound}}{}^2\mathbf{A} = \mathbf{Ch}\ \mathbf{A}, \qquad (1)$$

where ρ, V_{sound}, and $\mathbf{A}$ are density, sound velocity, and the mode polarization vector, respectively. $\mathbf{Ch}$ is a 3×3 matrix. The sound velocity can be obtained by assuming a sine dispersion relation. All the obtained peak energies for longitudinal modes and their momentum transfers between 1.5 and 5.5 nm^{-1} were performed with weighted fitting by one sine function in order to determine q_{max} for a compressed wave velocity (see Fig. S1 in supplementary information). Transverse modes were also treated as the same as the longitudinal modes. The values

Table 1
Experimental conditions with crystal parameters and densities.

Run #	$\lambda_{\mathrm{before}}/\lambda_{\mathrm{after}}$ [nm]	$P^{a}_{\mathrm{before}}/P^{a}_{\mathrm{after}}$ [GPa]	P [GPa]	a [Å]	V [Å^3]	ρ [g/cm^3]
Pt001		0.0001	0.0001	3.92268(4)	60.360(2)	21.468(1)
Pt002	694.63/694.62	0.96/0.93	0.95(2)	3.9188(3)	60.179(12)	21.532(4)
Pt003	696.44/696.44	5.99/5.99	5.99(–)	3.8956(3)	59.117(14)	21.919(5)
Pt004	697.96/697.81	10.27/9.85	10.06(30)	3.8808(6)	58.449(26)	22.169(10)
Pt005	699.92/699.11	15.90/13.56	14.7(17)	3.8609(6)	57.551(25)	22.516(10)
Pt006	702.14/701.46	22.39/20.39	21.4(14)	3.8360(6)	56.447(27)	22.956(11)

[a] Pressures were measured before and after IXS measurements based on a ruby scale with $\lambda_0 = 694.28$ nm (Zha et al., 2000).

Table 2
Obtained elastic constants (C_{ij}, K_S, K_T, and G).

Run #	C_{11} [GPa]	C_{12} [GPa]	C_{44} [GPa]	K_S [GPa]	K_T[a] [GPa]	G_{VRH} [GPa]
Pt001	348.7(13)	245.8(13)	73.4(2)	280.1(9)	274.1(9)	63.7(5)
Pt002	361.4(26)	261.2(26)	74.9(4)	294.6(20)	288.3(19)	63.7(11)
Pt003	382.7(49)	269.3(49)	86.3(10)	307.1(36)	300.6(36)	72.9(21)
Pt004	393.2(102)	284.3(101)	89.0(44)	320.6(75)	313.8(74)	73.1(46)
Pt005	426.2(65)	308.4(65)	100.8(14)	347.6(49)	340.3(48)	81.2(29)
Pt006	496.2(62)	371.5(62)	118.6(10)	413.1(46)	404.5(46)	91.6(28)

Adiabatic bulk modulus (K_S) and shear modulus (G) were calculated from C_{ij}s. G_{VRH} means a Voigt–Reuss–Hill average.
[a] K_T values were calculated using α of $2.685(150)\cdot10^{-5}$ (Gschneidner, 1964), γ of 2.72(3) (Fei et al., 2007), and 300 K.

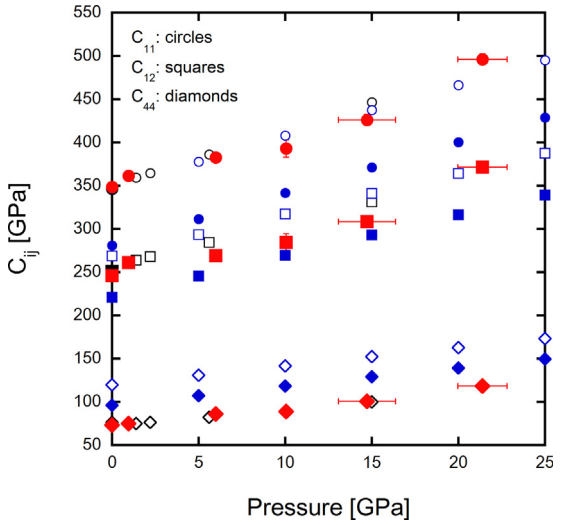

Fig. 3. Values of C_{ij} obtained in this study compared with previous studies. Circles, squares, and diamonds represent C_{11}, C_{12}, and C_{44}, respectively. Red symbols are C_{ij}s based on IXS, and blue open and solid symbols are those by theoretical calculation with LDA and GGA methods in this study, respectively. The black solid and the open symbols are from Macfarlane et al. (1965) and Menéndez-Proupin and Singh (2007), respectively. Macfarlane et al. (1965) obtained C_{ij} values at ambient pressure based on an ultrasonic method. On the other hand, Menéndez-Proupin and Singh (2007) obtained C_{ij} values by theoretical calculations.

of q_{max} were fixed in order to acquire a sound velocity at each data point. The detail of this analytical method is given in Appendix B. We used phonon modes with the wave vectors between 1.5 and 5.5 nm^{-1} in order to determine C_{ij} because the elastic line overlapped phonon modes below 1.5 nm^{-1}. The C_{ij}s were determined using data sets with between 44 and 101 of acoustic modes by fitting to Eq. (1).

2.2. First principles calculation

We also conducted first-principles calculations of the elastic constants for platinum. The Kohn-Sham equation was solved by means of the exact muffin-tin orbitals (EMTO) methods (Vitos et al., 2001). The local density approximation (LDA) or the generalized gradient approximation (GGA) was adopted for the exchange correlation function (Perdew and Wang, 1992; Perdew et al., 1996). The EMTO basis set included *s*, *p*, *d*, and *f* orbitals. The relativistic effects are taken into account within the scalar relativistic approximations. The total energy was calculated as a function of volume, and the calculation results were fitted to the third-order Birch–Murnaghan EOS to determine pressure and bulk modulus. The elastic constants can be obtained from the energy changes upon small strains (Vitos, 2007). The orthorhombic deformation was applied to calculate the tetragonal shear modulus $C' = (C_{11}-C_{12})/2$. The C_{11} and C_{12} elastic constants were then obtained from C' and the bulk modulus $K = (C_{11} + 2\,C_{12})/3$. Similarly, monoclinic distortion was used to calculate C_{44}.

3. Results and discussion

The experimental conditions and crystal parameters of Pt are summarized in Table 1 and obtained elastic constants are summarized in Table 2. As we observed that pressures based on the ruby scale were different before and after IXS measurements (see Table 1), experimental volumes obtained using Bragg reflections measured before, between, and after IXS scans were considered to be representative during IXS measurements. C_{ij}s obtained in this study are shown in Table 2 and observed and calculated sound velocities at ambient conditions are summarized in Table S1 in supplementary information. Experimental and calculated

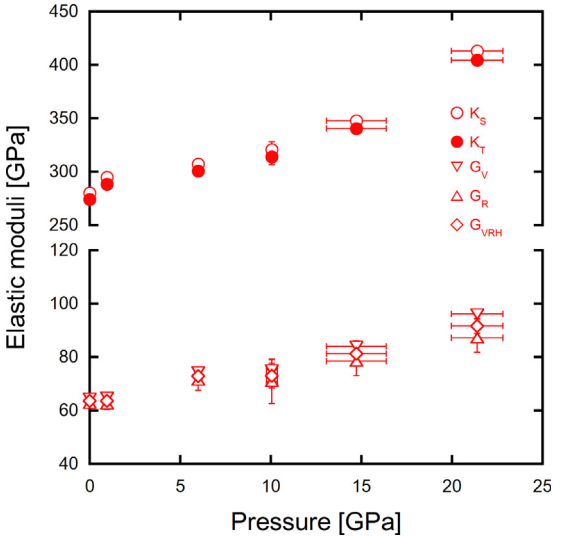

Fig. 4. Adiabatic and isothermal bulk moduli (K_T and K_S) and shear moduli (G) as a function of a pressure. Shear moduli (G_V, G_R, G_{VRH}) were calculated by Voigt, Reuss, and Voigt–Reuss–Hill averages.

Table 3
Volumes and pressures of Pt with pressures based on previous pressure scales.

Run #	V [Å^3]	P^a	P_{BM} (J82)	P_V (J82)	P_V (H89)	P_V (D04)	P_V (F07)	P_{BM} (F07)	P_V (M09)
Pt001	60.360(2)	0.0001	0	0	0	0	0	0	0
Pt002	60.179(12)	0.84(6)	0.82	0.81	0.8	0.83	0.84	0.84	0.83
Pt003	59.117(14)	6.09(10)	5.94	5.92	5.88	6.01	6.08	6.07	6
Pt004	58.449(26)	9.58(16)	9.46	9.44	9.39	9.57	9.67	9.65	9.55
Pt005	57.551(25)	14.65(21)	14.6	14.59	14.55	14.76	14.89	14.86	14.72
Pt006	56.447(27)	21.86(24)	21.61	21.62	21.62	21.81	21.98	21.92	21.75

Pressures are in GPa. P_{BM} and P_V represent pressures based on 3rd order Birch–Murnaghan EOS and Vinet EOS, respectively. J82: Jamieson et al. (1982), H89: Holmes et al. (1989), D04: Dewaele et al. (2004), F07: Fei et al. (2007), M09: Matsui et al. (2009).
[a] Pressures in this study were calculated with calculated $K_S = (1 + \alpha\ \gamma\ T)\ K_T$.

C_{ij}s in this study were plotted versus pressure in Fig. 3 together with those in previous studies (Macfarlane et al., 1965; Menéndez-Proupin and Singh, 2007). The present C_{ij}s increase monotonically with pressure as it can be easily seen from Fig. 3. The values of C_{11} and C_{44} are in good agreement with those obtained in previous studies. While values of C_{12} are slightly smaller between 5 and 15 GPa than those in the previous studies, they are generally consistent. The calculated C_{ij}s based on LDA show similar values to those of Macfarlane et al. (1965) obtained based on an ultrasonic method, and Menéndez-Proupin and Singh (2007) that also adopted LDA. On the other hand, the C_{ij}s calculated based on GGA are smaller than the previous studies, probably because the GGA method tends to underestimate elastic moduli as was pointed out by Dewaele et al. (2004). The present study gives the first experimental results of C_{ij} under pressure, which reasonably agree with the LDA calculations.

Fig. 4 shows adiabatic bulk moduli (K_S) and shear moduli (G) calculated using the C_{ij}s obtained in the present study. As can be seen from Fig. 4, K_S and G increase monotonically with pressure. Isothermal bulk moduli (K_T), also plotted in Fig. 4, were obtained using the thermodynamic relation as follows:

$$K_T = \frac{K_S}{1 + \alpha\ \gamma\ T}, \tag{2}$$

where α, γ, and T represent the thermal expansion coefficient, the Grüneisen parameter, and the absolute temperature, respectively. In this study, we assumed α to be independent of pressure and equal to $2.685(150)\cdot10^{-5}$ [K^{-1}] (Gschneidner, 1964) and $\gamma = \gamma_0(V/V_0)^q = 2.72(3) \times (V/V_0)^{0.5(5)}$ (Fei et al., 2007). Errors of K_T were calculated using errors of α, γ, and K_S. In order to calculate pressures, we used the definition of isothermal bulk modulus as follows:

$$K_T = -V\left(\frac{\partial P}{\partial V}\right)_T, \tag{3}$$

where K_T and P are isothermal bulk modulus and pressure, respectively. V is the volume at a given pressure. By integrating Eq. (3), experimental pressures can be calculated without any pressure scale. The pressures in this study were calculated using Eq. (4) and the trapezoidal rule as follows:

$$P = -\int_{V_0}^{V} \frac{K_T}{V}\,dV \approx \sum_i \left[\left(\left(\frac{K_T}{V}\right)_i + \left(\frac{K_T}{V}\right)_{i-1}\right)\frac{\Delta V}{2}\right], \tag{4}$$

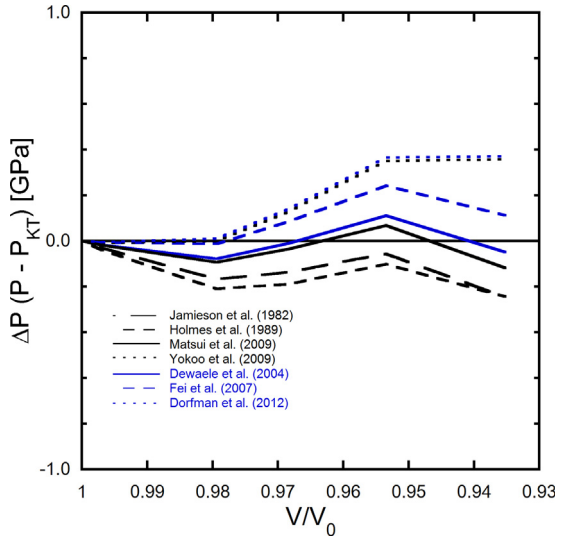

Fig. 5. Pressure differences between primary pressures in this study based on K_T and other scales.

where i represents a certain experimental condition. The calculated pressures are summarized in Table 3, which also includes the pressures acquired using the ruby scale and the previously reported EOSs of Pt. Fig. 5 displays the difference between experimental pressures determined based on Eq. (4) with K_T in the present study and those of other pressure scales (Pt), which are shown as a function of the normalized volume. Pressures acquired in this study are in good agreement with other pressure scales, as shown in Fig. 5.

In order to establish a primary pressure scale, we fitted third-order Birch–Murnaghan EOS (3BM) and Vinet EOS (V-EOS) to the P–V data (Birch, 1952; Vinet et al., 1987). The EOSs are expressed as follows, respectively:

$$P = \frac{3}{2}K_{T0}\left(\left(\frac{V_0}{V}\right)^{\frac{7}{3}} - \left(\frac{V_0}{V}\right)^{\frac{5}{3}}\right)\left[1 - \frac{3}{4}(4 - K')\left(\left(\frac{V_0}{V}\right)^{\frac{2}{3}} - 1\right)\right], \tag{5}$$

$$P = 3K_{T0}\left(\frac{V}{V_0}\right)^{\frac{-2}{3}}\left(1 - \left(\frac{V}{V_0}\right)^{\frac{1}{3}}\right)\exp\left[\frac{3}{2}(K' - 1)\left(1 - \left(\frac{V}{V_0}\right)^{\frac{1}{3}}\right)\right], \tag{6}$$

where K_{T0}, K', and V_0 represent the isothermal bulk modulus at 0 GPa, the pressure derivative of the bulk

Table 4
Parameters for the equation of state.

V_0	K_T	K'	EOS type	Ref.
60.366(13)	271.7(45)	5.35(47)	3BM	This study
60.367(13)	271.4(45)	5.43(47)	VEOS	This study
60.360(2)*	273.3(27)	5.23(35)	3BM	This study
60.360(2)*	273.0(28)	5.30(36)	VEOS	This study
60.360(2)*	274.1†	5.12(8)	3BM	This study
60.360(2)*	274.1†	5.17(8)	VEOS	This study
60.38*	268.2(30)	5.63(40)	3BM	This study
60.38*	268.0(30)	5.70(39)	VEOS	This study
60.38*	270.3(1)	5.267(4)	3BM	Jamieson et al. (1982)[a]
60.38*	268.9(2)	5.48(1)	VEOS	Jamieson et al. (1982)[a]
60.38*	266	5.81	VEOS	Holmes et al. (1989)
60.38*	273.6(20)	5.23(8)	VEOS	Dewaele et al. (2004)
60.38*	277	4.95(2)	3BM	Fei et al. (2007)
60.38*	277	5.08(2)	VEOS	Fei et al. (2007)
60.38*	276.07	5.3	VEOS	Dorogokupets and Oganov (2007)
60.38*	272.8(22)	5.22(10)	VEOS	Zha et al. (2008)[b]
60.38*	273	5.2	VEOS	Matsui et al. (2009)
60.55	276.4	5.48	VEOS	Yokoo et al. (2009)
60.38*	277	5.43(2)	VEOS	Dorfman et al. (2012)
60.38*	275.3	5.28	VEOS	Sokolova et al. (2013)

3BM: third-order Birch–Murnaghan EOS, VEOS: Vinet EOS.
* V_0 was fixed during the EOS fitting.
† K_T was fixed at a value obtained from K_S in ambient conditions.
[a] EOSs were re-fitted based on their PV data.
[b] EOS was re-fitted based on their PV data with Fei et al. (2007) and Dewaele et al. (2004).

modulus at 0 GPa, and the volume at 0 GPa. P and V are the pressure and volume of Pt at the pressure. The fitting parameters of K_{T0}, K', and V_0 are summarized in Table 4, with previous studies. The fitting results of this dataset with fixing V_0 show that K_{T0} of 273(3) GPa is in good agreement with the K_{T0} value of 274(1) GPa obtained from the K_S value at ambient pressure through the IXS measurements in this study and the previously reported value of 277 GPa based on ultrasonic measurements (Macfarlane et al., 1965). Fig. 6 illustrates the pressure differences between the present pressure scale based on V-EOS, with K_T = 274.1 GPa and K' = 5.17 and the previously reported V-EOSs up to 400 GPa. Our pressure scale is excellently consistent with that of Matsui et al. (2009) based on shock experiment data and is in good agreement with the Fei and Dewaele scales. At the same time, pressures of the Dorfman, Holems, Jameison, and Yokoo scales are considerably higher than ours over the whole range, up to 400 GPa.

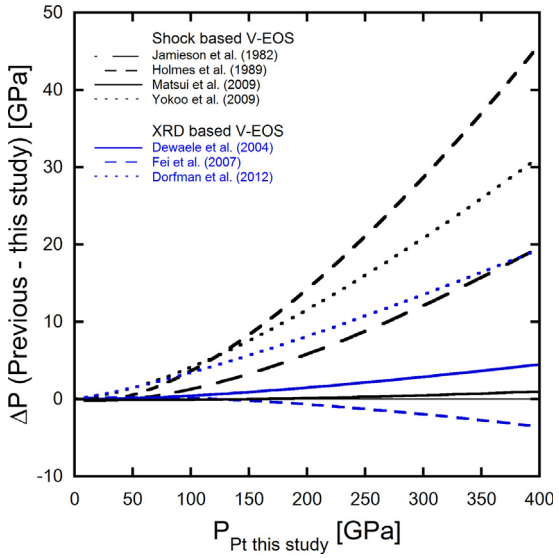

Fig. 6. Pressure differences between the Pt scale in this study and previous studies. The pressures based on our study were calculated using Vinet EOSs with V_0 = 60.360 Å^3, K_T = 274.1 GPa, and K' = 5.17. Parameters of Vinet EOSs for previous studies are summarized in Table 4.

4. Conclusion

We measured the IXS spectra of a single crystal of Pt from 1 bar to 20 GPa. The volumes of the sample were also measured using Bragg reflections before, between, and after IXS scans at each pressure point. The sound velocities of Pt were calculated using the sine dispersion relation. The parameters q_{max} for longitudinal and transversal modes were determined by fitting all peak energies of longitudinal or transversal modes to a single sine function between momentum transfers of 1.5 and 5.5 nm^{-1}. The q_{max} values were fixed during C_{ij} optimization. The C_{ij}s acquired using the sine relation are consistent with those based on the ultrasonic method and the calculation with LDA. As an implication, we established the primary pressure scale for Pt. Our pressure scale showed excellent agreement with the pressure scale suggested by Matsui et al. (2009) and is consistent with those by Dewaele et al. (2004) and Fei et al. (2004, 2007). On the other hand, pressure scales by Jamieson et al. (1982), Holmes et al.

(1989), Yokoo et al. (2009), and Dorfman et al. (2012) are significantly higher than the scale of the present work.

Acknowledgments

This work was supported by JSPS KAKENHI Grant Number 15H02128 to A.Y. S.K. was partly supported by JSPS KAKENHI Grant Numbers 26247089, 15H05831, and 16K13902. S.K. thanks M. Polovinka for editing the English text. The experiments were conducted under a contract at SPring-8 (proposal numbers 2016B1313 and 2017A1266). We appreciated discussions with Prof. Mashimo on V_P and V_S at ambient pressure.

Appendix A. Supplementary data

Supplementary data associated with this article can be found, in the online version, at https://doi.org/10.1016/j.crte.2018.11.003.

References

Baron, A.Q.R., 2016. High-Resolution Inelastic X-Ray Scattering I&II. In: Jaeschke, E., Khan, S., Schneider, J.R., Hasting, J.B. (Eds.), Synchrotron Light Sources and Free-Electron Lasers. Springer International Publishing [See also arXiv : 1504.01098v2], pp. 1643–1757.

Baron, A.Q.R., Tanaka, Y., Goto, S., Takeshita, K., Matsushita, T., Ishikawa, T., 2000. An X-ray scattering beamline for studying dynamics. J. Phys. Chem. Solids 61, 461–465.

Birch, F., 1952. Elasticity and constitution of the earth's interior. J. Geophys. Res. 57 (2), 227–286.

Dewaele, A., Loubeyre, P., Mezouar, M., 2004. Equation of state of six metals above 94 GPa. Phys. Rev. B 70, 094112.

Dorfman, S.M., Prakapenka, V.B., Meng, Y., Duffy, T.S., 2012. Intercomparison of pressure standards (Au, Pt, Mo, MgO, NaCl and Ne) to 2.5 Mbar. J. Geophys. Res 117, B08210.

Dorogokupets, P.I., Oganov, A.T., 2007. Ruby, metals, and MgO as alternative pressure scales: A semiempirical description of shock-wave, ultrasonic, x-ray, and thermochemical data at high temperatures and pressures. Phys. Rev. B 75, 024115.

Fei, Y., Li, J., Hirose, K., Minarik, W., Van Orman, J., Sanloup, C., van Westrenen, W., Komabayashi, T., Funakoshi, K., 2004. A critical evaluation of pressure scales at high temperatures by in situ X-ray diffraction measurements. Phys. Earth Planet. Inter. 143–144, 515–526.

Fei, Y., Ricolleau, A., Frank, M., Mibe, K., Shen, G., Prakapenka, V., 2007. Toward an internally consistent pressure scale. Proc. Natl. Acad. Sci. U S A 104 (22), 9182–9186.

Fukui, H., Katsura, T., Kuribayashi, T., Matsuzaki, T., Yoneda, A., Ito, E., Kudoh, Y., Tsutsui, S., Baron, A.Q.R., 2008. Precise determination of elastic constants by high-resolution inelastic X-ray scattering. J. Synchr. Rad. 15, 618–623.

Gschneidner Jr., K.A., 1964. Physical Properties and Interrelationships of Metallic and Semimetallic Elements. Solid State Phys. 16, 275–426.

Holmes, N.C., Moriarty, J.A., Gathers, G.R., Nellis, W.J., 1989. The equation of state of platinum to 660 GPa (6.6 Mbar). J. Appl. Phys. 66 (7), 2962–2967.

Ishikawa, D., Uchiyama, H., Tsutsui, S., Fukui, H., Baron, A.Q.R., 2013. Compound focusing for hard-X-ray inelastic scattering. In: Proc. SPIE 8848. .

Jamieson, J.C., Fritz, J.N., Manghnani, M.H., 1982. Pressure measurement at high temperature in X-ray diffraction studies: Gold as a primary standard. In: Akimoto, S., Manghnani, M.H. (Eds.), High-Pressure Research in Geophysics. Center for Academic Publications, Tokyo, pp. 27–48.

Macfarlane, R.E., Rayne, J.A., Jones, C.K., 1965. Anomalous temperature dependence of shear modulus C_{44} for platinum. Phys. Lett. 18 (2), 91–92.

Marsh, S.P., 1980. LASL Shock Hugoniot Data. University of California Press.

Matsui, M., Ito, E., Katsura, T., Yamazaki, D., Yoshino, T., Yokoyama, A., Funakoshi, K., 2009. The temperature-pressure-volume equation of state of platinum. J. Appl. Phys. 105, 013505.

Menéndez-Proupin, E., Singh, A.K., 2007. Ab initio calculations of elastic properties of compressed Pt. Phys. Rev. B 76, 054117.

Perdew, J.P., Burke, K., Ernzerhof, M., 1996. Generalized gradient approximation made simple. Phys. Rev. Lett. 77 (18), 3865.

Perdew, J.P., Wang, Y., 1992. Accurate and simple analytic representation of the electron-gas correlation energy. Phys. Rev. B 45 (23), 13244.

Sakai, T., Takahashi, S., Nishitani, N., Mashino, I., Ohtani, E., Hirao, N., 2014. Equation of state of pure iron and $Fe_{0.9}Ni_{0.1}$ alloy up to 3Mbar. Phys. Earth Planet. Inter. 228, 114–126.

Sokolova, T.S., Dorogokupets, P.I., Litasov, K.D., 2013. Self-consistent pressure scales based on the equations of state for ruby, diamond, MgO, B2-NaCl, as well as Au, Pt, and other metals to 4 Mbar and 3000 K. Russian Geol. Geophys. 54, 181–199.

Tateno, S., Hirose, K., Ohishi, Y., Tatsumi, Y., 2010. The structure of iron in Earth's inner core. Science 330, 359–361.

Tateno, S., Kuwayama, Y., Hirose, K., Ohishi, Y., 2015. The structure of Fe-Si alloy in Earth's inner core. Earth Planet. Sci. Lett. 418, 11–19.

Tsuchiya, T., Kawamura, K., 2002. First-principles electronic thermal pressure of metal Au and Pt. Phys. Rev. B 66, 094115.

Yokoo, M., Kawai, N., Nakamura, K.G., Kondo, K., Tange, Y., Tsuchiya, T., 2009. Ultrahigh-pressure scales for gold and platinum at pressures up to 550 GPa. Phys. Rev. B 80, 104114.

Vinet, P., Ferrante, J., Rose, J.H., Smith, J.R., 1987. Compressibility of solids. J. Geophys. Res. 92 (B9), 9319–9325.

Vitos, L., 2007. Computational quantum mechanics for materials engineers: the EMTO method and applications. Springer Science & Business Media.

Vitos, L., Abrikosov, I.A., Johansson, B., 2001. Anisotropic lattice distortions in random alloys from first-principles theory. Phys. Rev. Lett. 87 (15), 156401.

Yoneda, A., Fukui, H., Gomi, H., Kamada, S., Xie, L., Hirao, N., Uchiyama, H., Tsutsui, S., Baron, A.Q.R., 2017. Single crystal elasticity of gold up to ~20 GPa: Bulk modulus anomaly and implication for a primary pressure scale. Jp. J. Appl. Phys. 56, 095801.

Zha, C.S., Mao, H.K., Hemley, R., 2000. Elasticity of MgO and a primary pressure scale to 55 GPa. Proc. Natl. Acad. Sci. USA 97 (25), 13494–13499.